Resonance structure in the $4s^2(^1S_0) \rightarrow 4s4p(^3P_{0,1,2})$ electron-impact excitation of Kr^{6+}

T. W. Gorczyca and M. S. Pindzola
Department of Physics, Auburn University, Auburn, Alabama 36849

N. R. Badnell
Department of Physics and Applied Physics, University of Strathclyde, Glasgow, G4 0NG, United Kingdom

D. C. Griffin
Department of Physics, Rollins College, Winter Park, Florida 32789

(Received 23 August 1994)

We present Breit-Pauli R-matrix results for the resonance-enhanced $4s^2(^1S_0) \rightarrow 4s4p(^3P_{0,1,2})$ excitation cross section in Kr^{6+}. A comparison with a recent merged-beams experiment [Bannister *et al.*, Phys. Rev. Lett. **72**, 3336 (1994)] is made in the near-threshold region. From a 14-level calculation, we find fairly good agreement. The resonance structure in this region is predominantly due to $4s4p(^1P)n\ell(n = 9, 10)$ contributions, which are strongly perturbed by the $4s4d4f$ configuration. A sensitivity of the resulting cross section to the exact positions of these perturber resonances is demonstrated by varying the $4s4d(^{1,3}D)$ target thresholds.

PACS number(s): 34.80.Kw

I. INTRODUCTION

Recently, Bannister *et al.* reported measurements of absolute total cross sections for electron-impact excitation of an intercombination transition to a nonradiating state of an atomic ion [1]. The specific excitation was $4s^2(^1S) \rightarrow 4s4p(^3P)$ in Kr^{6+}, for which large enhancement due to dielectronic-capture resonances was observed in the near-threshold region. From a theoretical standpoint, one expects the calculation of such resonance-enhanced cross sections to be complicated by interference effects between various Rydberg series. A recent study of the similar $3s^2(^1S) \rightarrow 3s3p(^3P)$ excitation in Mg-like ions [2–4] showed not only that there was strong interference between resonance series, but also that the resulting cross section was quite sensitive to the exact positions of the perturbing resonances; in some cases, small changes in the resonance positions led to order-of-magnitude changes in the resonant cross section.

The present excitation in Kr^{6+} is further complicated by the existence of a full $3d$ subshell, which makes it extremely difficult to accurately describe the Kr^{6+} target states and even more difficult for the Kr^{5+} resonance states. Also, relativistic operators are responsible for roughly 1 eV shifts in the relative target energies and there is a 1 eV fine-structure splitting between the $4s4p(^3P_{0,1,2})$ levels, necessitating a Breit-Pauli treatment of the target states. Consequently, fully converged results for this resonance process are not to be expected beforehand. Nonetheless, it is of interest to study this excitation in order to classify the observed experimental resonance structure [1] and, guided by such data, assess the accuracy of the present theoretical treatment in light of the above considerations. We thus utilized the R-matrix method [5,6], with the inclusion of a Breit-Pauli Hamiltonian [7,8], as a means of studying this excitation.

The remainder of the paper is as follows. In Sec. II the atomic structure of the Kr^{6+} target states is presented, where discrepancies as large as 0.5 eV exist compared to spectroscopic values. Our means of correcting this discrepancy, an energy-shifting procedure, is described in Sec. III, and the difficulties of this method are discussed in relation to the present calculations. Section IV gives our results from various Breit-Pauli R-matrix scattering calculations, followed by concluding remarks in Sec. V.

II. Kr^{6+} TARGET DESCRIPTION

The eight lowest-lying states of Kr^{6+} (in LS coupling) are $4s^2(^1S)$, $4s4p(^{3,1}P)$, $4p^2(^3P, ^1D, ^1S)$, and $4s4d(^{3,1}D)$, which give rise to 14 fine-structure levels. Higher states will not be considered in the present treatment. We used the multi-configuration Hartree-Fock (MCHF) computer package of Froese-Fischer [9] in order to produce appropriate target orbitals and perform final configuration-interaction (CI) calculations. The CI was computed in intermediate coupling including mass-velocity, one-body Darwin, and spin-orbit operators in the Hamiltonian. The first seven orbitals $1s$, $2s$, $2p$, $3s$, $3p$, $3d$, and $4s$ were generated from a single-configuration Hartree-Fock (HF) calculation for the energy of the $4s^2(^1S)$ ground state. The excited-state orbitals $4p$ and $4d$ were then determined by performing frozen-core HF calculations for the average energy of the $4s4p$ and $4s4d$ configurations, respectively. Given this set of orbitals, improved energies were obtained by allowing CI of the form $4s^2 + 4p^2$ in the ground and excited $^1S_0$ levels and $4s4p + 4p4d$ in the $^{3,1}P^0_J$ levels. The $4s4d$ levels should be treated in a similar fashion by allowing

double-promotion CI with the $4p4f$ configuration, but, for reasons to be discussed in Sec. III, including a $4f$ orbital in the target description severely complicates the scattering problem when threshold energies are adjusted. We therefore omit the $4f$ orbital from the target-orbital basis.

The resulting energies from this Breit-Pauli CI calculation are listed in Table I compared to the latest experimental values [10,11]. The fine-structure splitting between the $4s4p(^3P_0)$ and $4s4p(^3P_2)$ levels is about 1 eV, indicating that an intermediate-coupled formulation of the problem is warranted, since the experimental energy resolution is 0.2 eV. Also, the discrepancy between theoretical and experimental energies is about 0.5 eV in some cases. The CI basis described above is somewhat limited, of course, and one may ask what could be done to improve the theoretical energies. In a study of the $4s^2(^1S) \rightarrow 4s4p(^1P)$ oscillator strengths in the zinc isoelectronic sequence, Froese-Fischer and Hansen [12] found that an extremely large set of pseudo-orbitals and configurations were required in order to obtain converged nonrelativistic MCHF energies. In a similar manner, we expanded the above basis to include $4f$, $\overline{5s}$, $\overline{5p}$, and $\overline{5d}$ orbitals, where the overbars denote pseudo-orbitals. Also, many more configurations were included, particularly the important $4p4f$ mentioned in the preceding paragraph, and configurations obtained by promoting out of the $3d$ subshell. With this enlarged basis, it was possible to get the $4s^2(^1S_0) \rightarrow 4s4p(^1P_1)$ energy to within 0.1 eV of experiment, but the $4s^2(^1S_0) \rightarrow 4s4p(^3P_J)$ energies were still about 0.4 eV lower than experiment. This indicated that the absolute energies of the singlet states were not as converged as the triplet states.

Thus the end result of greatly increasing the orbital and configuration bases is a minor improvement in the energies. As will be discussed in the next section, the energy-adjustment procedure becomes less reliable as the basis size increases and so we chose to limit the basis to the original, smaller set.

TABLE I. Breit-Pauli energies for Kr^{6+} (eV).

No.	Level		Theory	Experiment
1	$4s^2$	$^1S_0$	0.0	0.0
2	$4s4p$	$^3P_0$	14.05	14.55[a]
3		$^3P_1$	14.35	14.89[a]
4		$^3P_2$	15.03	15.69[a]
5		$^1P_1$	21.49	21.18[a]
6	$4p^2$	$^3P_0$	33.86	34.08[b]
7		$^1D_2$	34.13	34.35[b]
8		$^3P_1$	34.31	34.64[b]
9		$^3P_2$	35.18	35.73[b]
10		$^1S_0$	41.10	40.98[b]
11	$4s4d$	$^3D_1$	43.16	43.39[a]
12		$^3D_2$	43.21	43.45[a]
13		$^3D_3$	43.29	43.53[a]
14		$^1D_2$	48.34	47.05[a]

[a] Reference [10].
[b] Reference [11].

III. SHIFTING THRESHOLD ENERGIES WITHIN THE *R*-MATRIX METHOD

As pointed out in the preceding section, the theoretical target energies disagree with experimental values by as much as 0.5 eV. Using these inaccurate energies would likewise yield inaccurate resonance positions. The quantum-defect formula $E_n = E_{\text{thresh}} - z^2/2(n-\mu)^2$ gives the position of a Rydberg resonance with principle quantum number n attached to an excited state of threshold energy E_{thresh} and μ is the quantum defect. If one expects to line up theory with experiment, then one must adjust the theoretical values. The method we used has been described previously [13], but we highlight the key features below in order to point out the approximations invoked in the present scattering calculation.

In the standard formulation of the R-matrix method [5,6], the wave function inside the R-matrix box is expanded in the basis

$$\Psi_k^{N+1} = \mathcal{A} \sum_{ij} c_{ijk} \Psi_i^N u_{ij} + \sum_{\alpha} d_{\alpha k} \chi_\alpha^{N+1} , \tag{1}$$

where Φ_i^N is the target wave function for the ith target state times the spatial and spin parts of the colliding electron, u_{ij} are the continuum-orbital basis functions, $\mathcal{A}$ is the antisymmetrizing operator, and χ_α^{N+1} are square-integrable functions necessary to compensate for the enforced orthogonality

$$\langle u_{ij} | P_{nl} \rangle = 0 , \tag{2}$$

where P_{nl} is a target orbital. The functions χ_α^{N+1} are usually all $(N+1)$-electron configurations derived from the coupling of any target orbital P_{nl} to any N-electron configuration contained in the Φ_i^N target description. The resulting R-matrix Hamiltonian takes the form

$$H_{kk'} = \langle \Psi_k^{N+1} | \mathcal{H} | \Psi_{k'}^{N+1} \rangle \tag{3}$$

$$= \begin{pmatrix} H^{cc} & H^{cb} \\ H^{bc} & H^{bb} \end{pmatrix} , \tag{4}$$

where the superscripts c and b denote continuum or bound elements, i.e., the first or second term on the right-hand side of Eq. (1). The energy-shifting procedure consists of adding a diagonal matrix to the continuum-continuum block of the Hamiltonian H^{cc}, the components of which are given by the difference in theoretical and experimental energies, thereby ensuring correct target thresholds for the scattering process. In other words, the following transformation takes place:

$$\langle \Psi_i^N u_{ij} | \mathcal{H} | \Psi_{i'}^N u_{i'j'} \rangle \rightarrow \langle \Psi_i^N u_{ij} | \mathcal{H} | \Psi_{i'}^N u_{i'j'} \rangle + \delta_{ii'} \delta_{jj'} \{ E_i(\text{expt}) - E_i(\text{theor}) \} . \tag{5}$$

We note that although this adjustment corrects the target thresholds, and therefore the positions of resonances due to high-lying Rydberg states which converge to this corrected threshold, lower-lying resonances, namely, those that are described predominantly by the χ_α^{N+1}

functions, are not shifted. While we could have shifted these states as well by adding a correction to the H^{bb} part of the Hamiltonian, it is unclear how these lower-lying states should be treated. They are Kr^{5+} satellite states, for which no experimental energy levels exist. And Sec. II showed that we could not converge our Kr^{6+} relative energies, so that theoretically determining the positions of the Kr^{5+} states, even with a huge basis expansion, is unreliable. We could shift them by considering their Kr^{6+} parent, but such a classification becomes ambiguous in general, since, for example, the $4s4p4d$ configuration could be regarded as a $4d$ orbital coupled to a $4s4p$ parent or a $4p$ orbital coupled to a $4s4d$ parent. And these low-lying states are not necessarily best described by a valence orbital coupled to a parent state to begin with.

In view of these difficulties, we wish to minimize the number of orbitals and configurations necessary in the target description, thereby minimizing the number of such $(N+1)$-electron states, χ_α^{N+1}, that are required. Thus the resonances will be described by Rydberg orbitals, determined variationally within the R-matrix calculation, attached to the shifted target thresholds. It is for this reason that the $4f$ orbital was not included, even though $4p4f$ mixing with the $4s4d$ states is appreciable. Otherwise, resonances of the form $4s4d4f$ would be described as an $(N+1)$-electron, unshifted state. Similarly, pseudo-orbitals such as $\overline{5s}$, $\overline{5p}$, and $\overline{5d}$, which correct the term-dependent and relaxation effects of the target states, as mentioned in Sec. II, were not included.

IV. BREIT-PAULI CALCULATIONS

In this section we present our results for the near-threshold resonance structure of Kr^{6+}. Specifically, we will be looking in the 14.5–16.5 eV range, for which experimental data are available [1]. By applying a simple quantum-defect formula to the target thresholds $E_n = E_{\rm thresh} - z^2/2(n-\mu)^2$ and using the experimental energies given in Table I, one may predict the possible resonances in this region to be categorized according to Table II. In order to estimate the importance of each of these, we performed a series of calculations including only certain target levels, which therefore considered contributions from only certain of these resonances. From an R-matrix calculation including just the lowest four levels listed in Table I, we found a negligible contribution; that is, the $4s4p(3P_{1,2})n\ell$ resonances alone were quite small. But these resonances will be addressed shortly when other target levels are included.

TABLE II. Possible resonances in the near-threshold region (14.5 eV< E <16.5 eV).

Configuration	Principal quantum number
$4s4p(^3P_{1,2})n\ell$	$20 \le n < \infty$
$4s4p(^1P_1)n\ell$	$n = 9,10$
$4p^2n\ell$	$n = 5$
$4s4dn\ell$	$n = 4$

We investigated the $4s4p(^1P_1)n\ell$ resonance contributions within a five-level calculation including the $4s4p(^1P_1)$ target level. The results for this run are shown by the dotted curve in Fig. 1 compared to experiment. We point out that the experimental data points [1] have been shifted to lower energies by an amount $\Delta E = E_{^3P_1} - E_{\rm av} = -0.4$ eV, where $E_{\rm av}$ is the level-averaged energy of the $4s4p(^3P)$ configuration. This is because the data points in Ref. [1] were adjusted so that the onset for excitation occurred at $E = E_{\rm av}$. We have found, however, that excitation to the $^3P_1$ level dominates the sum of excitations to all three J levels, that is, the onset for excitation actually occurs at the $^3P_1$ threshold.

The large feature at 15 eV is due to $4s4p(^1P_1)9\ell$ resonances and that at 16.2 eV is due to $4s4p(^1P_1)10\ell$ resonances. It appears that the measured cross section is dominated by these two sets of resonances. In order to investigate the importance of the $4p^2n\ell$ resonances, a nine-level calculation, which excluded the $4s4p(^1P_1)$ target level, was performed and the cross section was again insignificant. But a ten-level calculation obtained by adding the $4s4p(^1P_1)$ target level gave a noticeably different profile for the second feature at 16.2 eV (see Fig. 1). A comparison of the two theoretical curves shows that the $4p^2n\ell$ configurations interact somewhat with the $4s4p(^1P_1)10\ell$ resonances.

We next looked at the $4s4d(^{1,3}D_J)n\ell$ resonances by including the four $4s4d(^1D_2,^3D_{1,2,3})$ levels in addition to the four lowest target levels. These (convoluted) results are shown in Fig. 2. The (unconvoluted) results for ex-

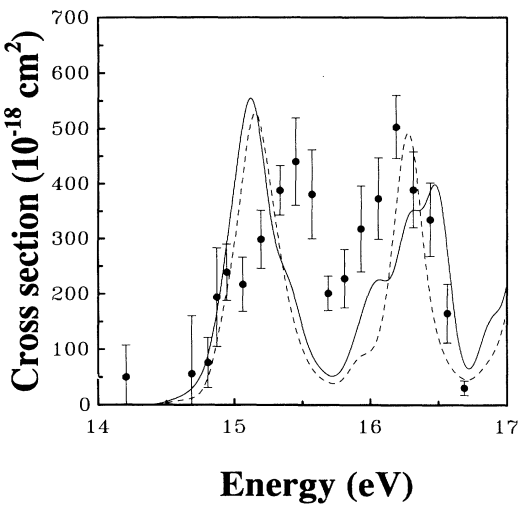

FIG. 1. Electron-impact excitation cross section for the $4s^2(^1S_0) \rightarrow \sum_J 4s4p(^3P_J)$ (J =0,1,2) transition in Kr^{6+}. Dotted line, five-level Breit-Pauli R-matrix calculation including target levels 1–5, with the thresholds adjusted to level-averaged experimental values, convoluted with a 0.2 eV full width at half maximum Gaussian; solid line: ten-level calculation including target levels 1–5 and 6–10; solid circles: merged-beams experimental values of Ref. [1], shifted by −0.4 eV.

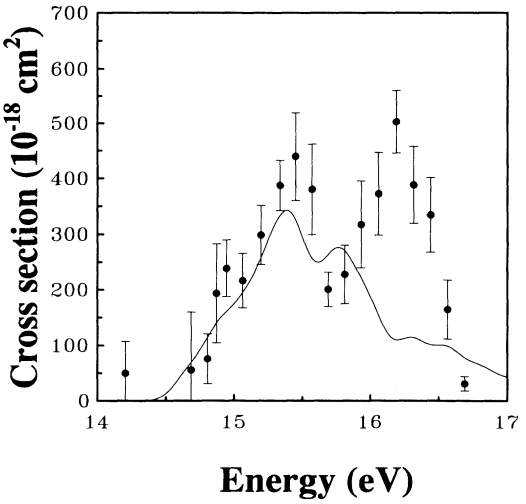

FIG. 2. Same as Fig. 1, except for an eight-level calculation including target levels 1–4 and 11–14.

citation to the $^3P_1$ level only, which was found to be the dominant excitation level of the three, are shown in Fig. 3(a). We show in Fig. 3(b) the same cross section from a four-level calculation, for which no $4s4d(^{1,3}D_J)n\ell$ resonances are present, and in Fig. 3(c) a seven-level calculation, which omits contributions from the $4s4p(^3P_2)n\ell$ resonances. Noting that these results are unconvoluted, it is seen from Fig. 3(c) that the $4s4d(^{1,3}D_J)n\ell$ resonances are extremely broad compared to the $4s4p(^3P_2)n\ell$ resonances of Fig. 3(b). Also, neglecting the small background cross section, the curve in Fig. 3(a) should be the sum of the curves in Figs. 3(b) and 3(c) if no interference occurs between the two. These results clearly indicate that the cross section in Fig. 3(a) results from broad perturbing resonances of the form $4s4d(^{1,3}D_J)n\ell$ interfering with the otherwise small Rydberg series of $4s4p(^3P_2)n\ell$ resonances converging to the $4s4p(^3P_2)$ threshold.

The precise configuration which composes this perturbing resonance may be identified as follows. First, we found that the broad feature in Fig. 3(c) is mostly due to odd-parity partial wave contributions, meaning that ℓ is odd. Second, according to Table II, we know that the principal quantum number can only be $n = 4$ in this energy region and thus $l \leq 3$. Third, the $4s4d4p$ resonances are found to be energetically located below all the $4s4p$ target levels. Since the perturbing resonances are of the form $4s4dn\ell$, this means that the only possible configuration consistent with the above facts is the $4s4d4f$ configuration. We point out that identification of the various resonances by energy position is easily done within perturbation theory using the computer program AUTOSTRUCTURE [14]. This method also detected strong resonance contributions from the $4s4d4f$ configuration. However, Fig. 3 demonstrates that strong interference effects exist between low-n and high-n resonances and for this reason, a detailed comparison between R-matrix and perturbation methods, which was done in the Mg-like study [2–4], was not attempted, since including these higher-order effects within the perturbative method

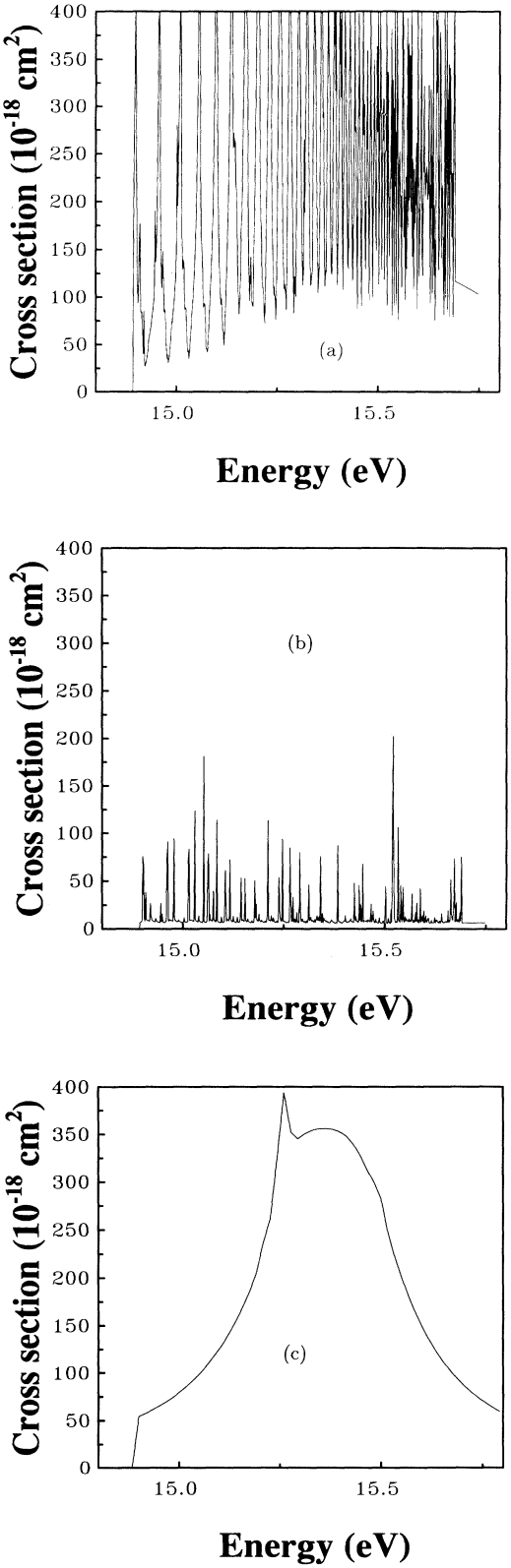

FIG. 3. Unconvoluted cross sections for excitation to just the $4s4p(^3P_1)$ target level in Kr^{6+}: (a) eight-level (targets 1–4 and 11–14), (b) four-level (targets 1–4), and (c) seven-level (targets 1–3 and 11–14) configurations.

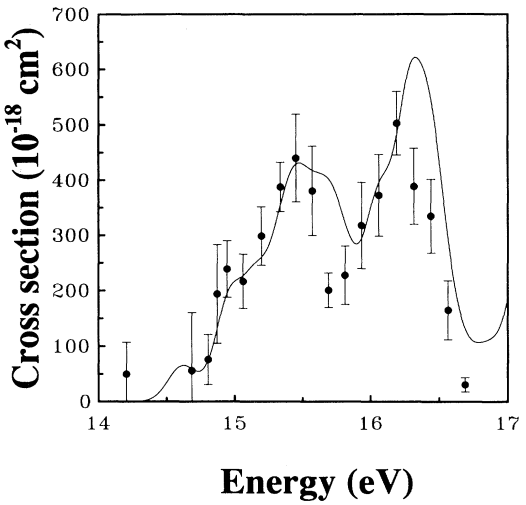

FIG. 4. Same as Fig. 1, except all 14 target levels were included.

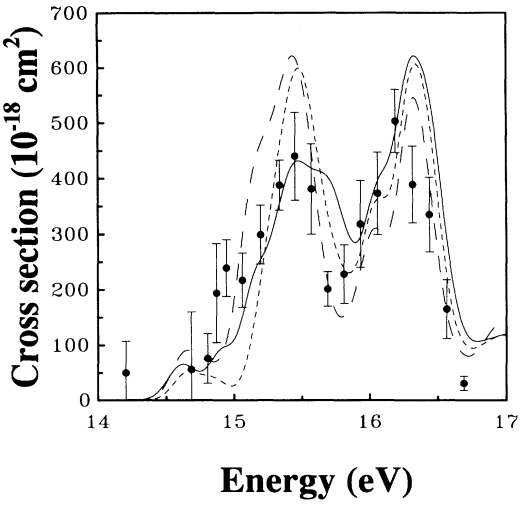

FIG. 5. Same as in Fig. 4, except that the $4s4d(^{1,3}D_J)$ thresholds have been shifted by 0.0 eV (solid curve), −0.2 eV (short-dashed curve), and −0.5 eV (long-dashed curve).

would have led to a tediously large calculation. The large enhancement in the cross section due to these $4s4d4f$ resonances also indicates that a converged cross section will be difficult to achieve since, as mentioned in Sec. II, the exact positions of these low-lying states are unknown experimentally and uncertain theoretically.

We finally performed a calculation including all 14 levels listed in Table I. The cross section, shown in Fig. 4, seems to agree fairly well with experiment, although this may be somewhat fortuitous considering the above arguments. We point out that our calculation was sensitive to the $(N+1)$-electron configurations included. Table III lists those used to produce the cross section in Fig. 4. Briefly, all $(N+1)$-electron configurations that can be constructed by coupling a $4s$, $4p$, or $4d$ orbital to an N-electron target configuration (those listed in Table I) were included. But it is unclear how the $4p4d$ configuration, which mixes into the $4s4p(^{1,3}P_J)$ target levels but is not a target itself, should be treated. If it were also an explicit target level, then the prescription would be to include the $4p4d^2$ $(N+1)$-electron configuration. However, no experimental values exist for the $4p4d$ threshold energies and determining these energies theoretically is unreliable. The theoretical positions of the $4p4d^2$ resonance positions are therefore inaccurate. We initially included these $4p4d$ N-electron target levels and their corresponding $4p4d^2$ $(N+1)$-electron configurations in a 14-level calculation anyway, without shifting these levels. We found in that case that the first peak was located −0.5 eV lower than in Fig. 4, but was roughly the same size and shape, indicating that the effect of including the $4p4d^2$ configuration was to just shift the $4s4p(^1P_1)9\ell$ resonances. But since the theoretical positions of these $4p4d^2$ resonances are highly suspect, we feel that a more reliable calculation is obtained by omitting these offending N-electron target levels and $(N+1)$-electron configurations altogether.

In regard to the inaccurate positions of low-lying perturbing resonances, the $4s4d4f$ positions are themselves questionable. These are described by a $4f$ valence orbital, variationally generated within the R-matrix code, attached to a shifted $4s4d$ target threshold, and then CI mixed with all other channels. Even though this description seems sufficient, the error in energy position, according to the quantum-defect formula, behaves as $\Delta E \sim Z^2/(n-\mu)^3$, so that the lower-lying resonances have larger uncertainties in their positions compared to the positions of, say, the higher-lying $4s4p(^1P_1)n\ell$ $(n = 9$ or 10) resonances. And since these resonances strongly perturb the $4s4p(^1P_1)(9,10)\ell$ resonances, there is a corresponding inaccuracy in the final resonance profile. In order to demonstrate the possible inaccuracies introduced into the calculation by incorrectly positioning the $4s4d4f$ resonances incorrectly, we artificially shifted all $4s4d(^{1,3}D_J)$ target levels. We show a family of curves in Fig. 5, for which these target levels were shifted from 0.0 eV, 0.2 eV, and 0.5 eV. The effect of shifting the target levels is to steadily increase the height of the 15.5 eV feature while decreasing the height of the 16.3 eV feature. This clearly indicates the extent to which the uncertainty in position of the $4s4d4f$ resonances affects the overall cross section.

TABLE III. $(N+1)$-electron configurations included in the final calculation.

$4s^24p$	$4s^24d$
$4s4p^2$	$4s4d^2$
$4p^3$	$4p^24d$
$4s4p4d$	

V. CONCLUSION

The recent experiment by Bannister *et al.* was the first measurement of strongly pronounced resonance structure

in an electron-ion excitation. We have shown that a Breit-Pauli R-matrix calculation has reasonably duplicated the measured resonance profile of the $4s^2(^1S_0) \rightarrow 4s4p(^3P_{0,1,2})$ electron-impact excitation cross section of Kr^{6+}, although the agreement may be somewhat fortuitous. The resulting resonance structure was shown to be sensitive to the exact position of the low-lying Kr^{5+} perturbing states, the correct positions of which are at this time uncertain, so that accurate theoretical predictions of the resonance profile are not at hand. Spectroscopic or converged theoretical values of these low-lying Kr^{5+} satellite states are thus highly desirable in order to allow a more sophisticated theoretical treatment of this excitation process. The present case of Kr^{6+} is complicated by the need to utilize an intermediate-coupling scheme, by the amount of correlation necessary to obtain converged target energies, and by the strong perturbing resonances, $4s4d4f$. Similar complications will be found in the theoretical determination of resonance structure associated with electron excitation of most heavy atomic ions.

ACKNOWLEDGMENTS

We would like to thank the members of the Iron Project for the use of their Breit-Pauli R-matrix programs. This work was supported in part by the U.S. Department of Energy, Office of Fusion Energy, under Contract No. DE-FG05-86-ER53217 with Auburn University and Contract No. DE-FG05-93ER54218 with Rollins College, and also by NATO Contract No. CRG 940134 with the University of Strathclyde.

[1] M. E. Bannister, X. Q. Guo, T. M. Kojima, and G. H. Dunn, Phys. Rev. Lett. **72**, 3336 (1994).
[2] N. R. Badnell, D. C. Griffin, T. W. Gorczyca, and M. S. Pindzola, Phys. Rev. A **48**, R2519 (1993).
[3] D. C. Griffin, M. S. Pindzola, F. Robicheaux, T. W. Gorczyca, and N. R. Badnell, Phys. Rev. Lett. **72**, 3491 (1994).
[4] N. R. Badnell, D. C. Griffin, T. W. Gorczyca, and M. S. Pindzola, Phys. Rev. A **50**, 1231 (1994).
[5] P. G. Burke and W. D. Robb, Adv. At. Mol. Phys. **11**, 143 (1975).
[6] P. G. Burke and K. A. Berrington, *Atomic and Molecular Processes: An R-Matrix Approach* (IOP, Bristol, 1993).
[7] N. S. Scott and P. G. Burke, J. Phys. B **13**, 4299 (1980).
[8] N. S. Scott and K. T. Taylor, Comput. Phys. Commun. **25**, 347 (1982).
[9] C. Froese Fischer, Comput. Phys. Commun. **64**, 369 (1991).
[10] A. Trigueiros, S.-G. Petterson, and J. G. Reyna Almandos, Phys. Scr. **34**, 164 (1986).
[11] E. H. Pinnington, W. Ansbacher, and J. A. Kernahan, J. Opt. Soc. Am. B **1**, 30 (1984).
[12] C. Froese Fischer and J. E. Hansen, Phys. Rev. A **17**, 1956 (1978).
[13] K. A. Berrington, J. Phys. B **18**, L395 (1985).
[14] N. R. Badnell, J. Phys. B **19**, 3827 (1986).